5-2011

Capturing Low Probability of Disease Dynamics in Coupled Populations

Jackson Burton
Montclair State University

MONTCLAIR STATE UNIVERSITY

CAPTURING LOW PROBABILITY BEHAVIOR OF DISEASE DYNAMICS IN COUPLED POPULATIONS

by

Jackson Burton

A Master's Thesis Submitted to the Faculty of

Montclair State University

In Partial Fulfillment of the Requirements

For the Degree of

Master of Science in with a Concentration in Pure and Applied Mathematics

May 2011

School College of Math and Sciences

Department Mathematical Sciences

[redacted]

Dr. Robert Prezant
Dean

5/2/11

May 2011

Thesis Committee:

[redacted]

Dr. Lora Billings
Thesis Sponsor

[redacted]

Dr. Diana Thomas
Committee Member

[redacted]

Dr. Eric Forgoston
Committee Member

[redacted]

Dr. Helen M. Roberts
Department Chair

ABSTRACT

Title of Thesis: CAPTURING LOW PROBABILITY BEHAVIOR OF DISEASE DYNAMICS IN COUPLED POPULATIONS

Jackson Burton, Master of Science, 2011

Thesis directed by: Dr. Lora Billings

Department of Mathematical Sciences

Researchers using mathematical models have made significant contributions to the field of epidemiology in recent years. These models have both explanatory and predicative power to describe disease dynamics. More recent work has considered multi-population models and the effects vaccinations have on the population as a whole. One such example can be seen in the West African country of Cameroon, which has two distinct patterns of measles outbreaks. By considering Cameroon as two subpopulations, a deterministic model is developed that includes the effect of vaccinations. Stability analysis is then performed on the model over a range of coupling and vaccination rates to establish thresholds between disease absence and persistence. Stochastic methods are then used to capture low probability events near these thresholds. We identified significant differences in vaccination rates predicted deterministically for disease absence versus vaccination rates that are effective at inducing disease absence.

CAPTURING LOW PROBABILITY BEHAVIOR OF DISEASE DYNAMICS IN COUPLED POPULATIONS

A THESIS

Submitted in partial fulfillment of the requirements

For the degree of Master of Science in Pure and Applied Mathematics

By

JACKSON BURTON

Montclair State University

Montclair, NJ

May 2011

Contents

List of Figures

List of Tables

1 Introduction

One common method to study diseases mathematically involves constructing compartmental models [1]. These models can be tailored to capture the most important dynamics in the spread of a disease of interest. Such models are useful for developing, testing, and implementing theories about disease dynamics. These models help give a clearer understanding of overall dynamics and can aid in developing optimal strategies for reducing disease transmission in populations [4]. Many compartmental models focus on the disease dynamics of a single population. However, we observe that most populations are not isolated but instead are linked by coupling, i.e the flux of individuals from one population to another. Because of this, we are interested in how coupling and vaccination affect the disease dynamics of distinct populations.

We consider a specific case involving the northern and southern regions of Cameroon. These two subpopulations display distinct patterns of outbreaks of measles. [2]. Measles is generally not a life threatening disease, although lack of adequate medical resources and sanitation has resulted in many deaths. This has been the case in both the northern and southern regions of Cameroon. To fight this, vaccination campaigns are in place to vaccinate children at a young age. However, even though vaccinations incur life long immunity, measles is nonetheless endemic [8].

Incidence has been particularly low for certain provinces in the north and south. However a new pattern of recent outbreaks are emerging. [2]. The country has attracted the attention of researches who are interested in evaluating the effectiveness the current vaccination campaigns. We are motivated to model the effects of coupling and vaccination on disease dynamics by developing a deterministic system of ordinary differential equations. Documented demographical data will be used for parameters, while other important parameters, namely the coupling and vaccination rates, will be analyzed over a range of values. Using stability analysis, we can establish bifurcations of disease absence versus disease persistence. These deterministic values of the bifurcation points will describe qualitative changes of the mean behavior of the system. To capture dynamics that can not be seen in a deterministic system, a stochastic representation of the model will be used to examine the behavior of the system near these bifurcation points. The primary goal is to establish differences between deterministic and stochastic threshold values for disease absence in terms of vaccination rates.

2 Compartmental Models

Compartmental models separate a population into mutually exclusive classes. An individual of the population is located in exactly one of them at any given time. The various epidemiological states are dependent upon the disease being modeled. Individuals with certain childhood diseases such as chicken pox, measles, and mumps for example, will go through four distinct disease states: susceptible, exposed, infected,

and recovered. The classes represent each of these states and the variables S, E, I and R are typically used to represent them. The variable S refers to the number of individuals who are susceptible to contracting the disease. E refers to the number of individuals who have contracted the disease but can not yet transmit it. I refers to the number of individuals who have contracted the disease and can transmit it, and R refers to the number of individuals who have recovered and are now immune from the disease.

Although many diseases have a latent period, they are much more difficult to perform analysis on. Because of that, we oftentimes will analyze a simpler compartmental model that uses the S, I, and R classes only. In fact much analysis has already been performed the Susceptible-Infected-Recovered (SIR) model [4].

2.1 The Basic SIR Model

The basic SIR compartmental model is used to describe an epidemic that occurs over a relatively short period of time within a population. The model was first introduced by Kermack and McKendrick [6] who were motivated by Bernoulli's work on smallpox deaths [9]. This model assumes the population is closed, i.e. individuals do not enter or leave a class via birth, death, or external migration. This is a reasonable assumption over a short time period. The SIR model is described by a system of differential equations describing the change in the number of individuals in each class over time. The system is given below:

$$\begin{aligned} \frac{dS}{dt} &= \frac{-\beta SI}{N}, \\ \frac{dI}{dt} &= \frac{\beta SI}{N} - \kappa I, \\ \frac{dR}{dt} &= \kappa I. \end{aligned} \tag{1}$$

Here, N denotes the population size and $\beta > 0$ describes the average number of contacts that can sufficiently transmit the disease per unit time. Thus $\beta I/N$ is the average number of contacts one susceptible will have with infectives per unit time, and $\beta SI/N$ describes the number of new infections per unit time. The rate of recovery is assumed to be exponentially distributed, i.e. individuals recover at a rate proportional to the population of infectives. Therefore the mean recovery period is κ^{-1} and we use κ to represent the average rate of recovery. The recovery rate is a biological parameter depending solely on the disease itself, whereas the contact rate depends on the disease as well as the population density and overall mixing.

An important fact about this model is that the population size, N, at any time is the sum of the number of individuals in each class. Therefore, since N is a constant quantity with $S + I + R = N$, then

$$\frac{dS}{dt} + \frac{dI}{dt} + \frac{dR}{dt} = \frac{dN}{dt} = 0. \tag{2}$$

As we make modifications to this model, we will ensure that the time derivative $dN/dt = 0$ for all $t \geq 0$. This result implies that the value of any one single class can be completely determined by the others. For example in the SIR model, $R = N - S - I$. This allows us to ignore analysis on the recovered class and reduces the model to a 2-dimensional system. We will employ this result for the remainder of the models used.

Although Eq. (1) cannot be solved in closed form, we can describe an epidemic from a qualitative perspective as follows. Note that $dS/dt < 0$ for all $t \geq 0$ and $dI/dt > 0$ implies

$$\frac{dI}{dt} = \frac{\beta SI}{N} - \kappa I = I\left(\frac{\beta S}{N} - \kappa\right) > 0. \tag{3}$$

Hence $dI/dt > 0$ if and only if $S > \kappa N/\beta$. Since S decreases for all t, I will eventually decrease and approach zero. Let $S(0) = S_0$. Then, if $S_0 < \kappa N/\beta$, then I decreases to zero monotonically. However, if $S_0 > \kappa N/\beta$, then $dI/dt > 0$ and I will first increase to a maximum at $S = \kappa N/\beta$ before decreasing to zero. This case illustrates an epidemic outbreak.

To determine the behavior of trajectories of Eq (1), we can analyze the relationship between S and I and consider

$$\frac{dI}{dS} = \frac{\beta SI/N - \kappa I}{-\beta SI/N}. \tag{4}$$

Solving by separation of variables yields

$$I = -S + \frac{\kappa N}{\beta} \ln S + c. \tag{5}$$

For any initial condition $(S(0), I(0)) = (S_0, I_0)$ we have

$$I = -S + \frac{\kappa N}{\beta} \ln S + I_0 + S_0 - \frac{\kappa N}{\beta} \ln S_0. \tag{6}$$

As mentioned above, the maximum number of infectives occurs at $S = \kappa N/\beta$ and thus

$$I_{max} = -\frac{\kappa N}{\beta} + \frac{\kappa N}{\beta} \ln \frac{\kappa N}{\beta} + I_0 + S_0 - \frac{\kappa N}{\beta} \ln S_0. \tag{7}$$

But, we also know that I approaches zero as time increases. Thus, we can describe

$$\lim_{t \to \infty} (S, I) = (\tilde{S}, 0) \tag{8}$$

with $\tilde{S}$ interpreted as the number of susceptibles who escaped infection. For any initial condition (S_0, I_0), the trajectory approaches $(\tilde{S}, 0)$ where $\tilde{S}$ is defined implicitly by

$$0 = -\tilde{S} + \frac{\kappa N}{\beta} \ln \tilde{S} + I_0 + S_0 - \frac{\kappa N}{\beta} \ln S_0. \tag{9}$$

We can numerically simulate trajectories of Eq. (1) using parameter values N, β, and κ from Table 1, given below. The parameter values used, although not

Table 1: Sample Parameter Values for SIR models

Parameter	Value	Units	Description
N	1000	people	Population size
β	200	year^{-1}	Contact rate
κ	100	year^{-1}	Recovery rate
μ	2	year^{-1}	Birth and death rate
v	$[0,1]$	per capita	Vaccination rate

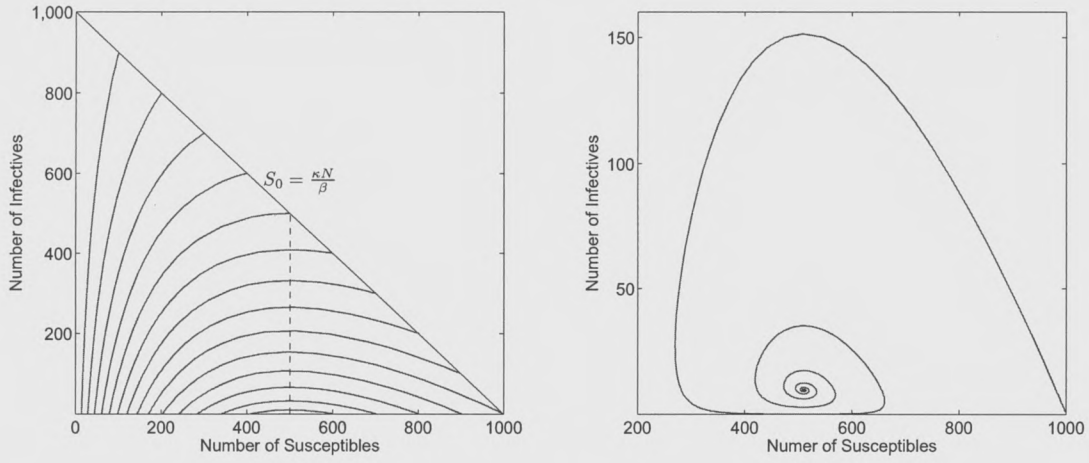

Figure 1: (a) Simulation of trajectories of the Basic SIR model. All trajectories with initial condition $S_0 > \kappa N/\beta$ first increases to a maximum given by Eq. (7). (b) Simulation of a single trajectory of the Basic SIR model with births and deaths. The limiting behavior is approaching $(\tilde{S}, \tilde{I})$, a stable spiral sink.

corresponding to a particular disease, fall within a reasonable range of real disease and demographic parameters. This has been done so that scales of plots will allow for clear graphical results. See Fig. 1(a) for a simulation of various trajectories of Eq. (1). The simulation was created using Matlab's ode45 differential equation solver, a Runga-Kutta 45 scheme [10]. Future simulations of models will all make use of the ode45 solver, and unless otherwise specified, no modifications or change of variables will be performed on the original systems.

The quantity $\beta S_0/(\kappa N)$ is a threshold quantity such that if $\beta S_0/(\kappa N) > 1$, then an outbreak will occur. On the other hand, if $\beta S_0/(\kappa N) < 1$ then no outbreak will occur. If we consider an almost completely susceptible population so that $S_0 \approx N$ and $I_0 \approx 0$, then the threshold quantity becomes β/κ. We define this quantity as the basic reproductive number R_0. Since β is the number of infections one infective makes per unit time and $1/\kappa$ is the mean length of the infective period, we interpret R_0 to be the number of secondary infections one infective produces in a completely susceptible population.

In summary, there have been two interpretations of the basic reproductive number although they refer to the same phenomena. The one interpretation describes

R_0 as a threshold value for which a disease will spread or fade out. The other interpretation describes R_0 as the number of secondary infections one infective can produce in a completely susceptible population. A central goal for the remainder of this paper is to define the basic reproductive number for modified models based off of Eq. (1) thus allowing us to characterize thresholds for differing disease dynamics.

2.2 The SIR Model with Births and Deaths

In order to model long term disease dynamics, we must include the events of birth and death in the SIR model. This will allow an influx of new susceptibles through birth and removal of susceptible, infected, and recovered individuals through death. This modification to the basic SIR model allows for an endemic state to exist, i.e. the state in which the disease persists. Let $\mu > 0$ represent both the birth and death rate, with μ^{-1} representing the average life span of an individual.

The SIR model with births and deaths is given by

$$\begin{aligned} \frac{dS}{dt} &= \frac{-\beta SI}{N} + \mu N - \mu S, \\ \frac{dI}{dt} &= \frac{\beta SI}{N} - \kappa I - \mu I, \\ \frac{dR}{dt} &= \kappa I - \mu R. \end{aligned} \tag{10}$$

Here, μN refers to the number of individuals who are born susceptible per unit time, while the terms μS, μI, and μR refer to the number of individuals who are removed from the classes due to natural death per unit time. This assumption that the birth and death rates are the same ensure that $dN/dt = 0$. Therefore, the population remains constant as before with $R = N - S - I$, and we do not need to consider R in our analysis.

For the remainder of the paper, maple will be used exclusively for all symbolic manipulation and computation. Setting the time derivatives in Eq. (10) equal to zero and solving yields two fixed points. One of the fixed points, $(S, I) = (N, 0)$, represents the disease free equilibrium (DFE), the state in which the disease is absent. The stability of the DFE can be determined by evaluating the Jacobian of the system at $(N, 0)$ and analyzing the eigenvalues. This linearization about the fixed point will characterize the stability.

Let $dS/dt = F_1(S, I)$, $dI/dt = F_2(S, I)$ and $\mathbf{F} = \langle F_1, F_2 \rangle$. The Jacobian of $\mathbf{F}$ is

$$J_{\mathbf{F}} = \begin{bmatrix} -\frac{\beta I}{N} - \mu & -\frac{\beta S}{N} \\ \frac{\beta I}{N} & \frac{\beta S}{N} - \kappa - \mu \end{bmatrix}. \tag{11}$$

The Jacobian evaluated at $(N, 0)$ is

$$J_{\mathbf{F}}|_{(N,0)} = \begin{bmatrix} -\mu & -\beta \\ 0 & \beta - \kappa - \mu \end{bmatrix}, \tag{12}$$

with eigenvalues

$$\begin{aligned} \lambda_1 &= -\mu, \\ \lambda_2 &= \beta - \kappa - \mu. \end{aligned} \tag{13}$$

In order for the DFE to be stable, the real parts of λ_1 and λ_2 must be negative. Clearly λ_1 and λ_2 are real values with $\lambda_1 < 0$. We see that $\lambda_2 < 0$ if and only if $\beta/(\kappa + \mu) < 1$. Therefore, if $\beta/(\kappa + \mu) < 1$, then the DFE becomes locally stable. We define $R_0 = \beta/(\kappa + \mu)$ as the threshold quantity for which the disease will die out or persist in the population. If $R_0 > 1$, then the DFE becomes unstable and the other fixed point

$$(\tilde{S}, \tilde{I}) = \left(\frac{N(\kappa + \mu)}{\beta}, \frac{\mu N(\beta - \mu - \kappa)}{\beta(\kappa + \mu)} \right) \tag{14}$$

becomes locally stable. This fixed point represents the endemic equilibrium (EE), the state in which the disease persists. In the case prior when $R_0 < 1$, the EE was unstable. The change in stability between the DFE and EE is a transcritical bifurcation. Transcritical bifurcations describe the interchange of stability between two fixed points, such as the instance where the DFE goes from stable to unstable resulting in the EE going from an unstable sink to stable sink. The bifurcations found in the remainder of this paper will all be transcritical bifurcations.

We can linearize about $(\tilde{S}, \tilde{I})$. The eigenvalues of the Jacobian evaluated at $(\tilde{S}, \tilde{I})$ are

$$\lambda_{1,2} = \frac{-\mu\beta \pm \sqrt{\mu[\beta^2\mu + 4(\kappa + \mu)^2(-\beta + \kappa + \mu)]}}{2(\kappa + \mu)}. \tag{15}$$

Clearly, both of these eigenvalues have negative real parts. Further, if $\beta^2\mu + 4(\kappa + \mu)^2(-\beta + \kappa + \mu) < 0$, then both eigenvalues are complex conjugate pairs. We can determine when this condition is true by considering

$$\begin{aligned} \beta^2\mu + 4(\kappa + \mu)^2(-\beta + \kappa + \mu) = 0 \quad &\Longrightarrow \\ \tfrac{\beta^2}{(\kappa+\mu)^2} - \tfrac{4(\beta-\kappa-\mu)}{\mu} = 0 \quad &\Longrightarrow \\ R_0^2 - \tfrac{4}{\mu}(\kappa + \mu)(R_0 - 1) = 0 \quad &\Longrightarrow \\ R_0^2 - \tfrac{4}{\mu}(\kappa + \mu)R_0 + \tfrac{4}{\mu}(\kappa + \mu) = 0 \quad &\Longrightarrow \\ R_0 = \tfrac{2\left(\kappa+\mu\pm\sqrt{\kappa(\mu+\kappa)}\right)}{\mu}. \end{aligned} \tag{16}$$

by the quadratic formula. Therefore, the eigenvalues are complex conjugate pairs when

$$\frac{2\left(\kappa + \mu - \sqrt{\kappa(\mu + \kappa)}\right)}{\mu} < R_0 < \frac{2\left(\kappa + \mu + \sqrt{\kappa(\mu + \kappa)}\right)}{\mu}. \tag{17}$$

We note that when

$$1 < R_0 < \frac{2\left(\kappa + \mu - \sqrt{\kappa(\mu+\kappa)}\right)}{\mu}, \tag{18}$$

then $(\tilde{S}, \tilde{I})$ is a stable sink. However, if Eq. (17) holds, then the fixed point $(\tilde{S}, \tilde{I})$ is a stable spiral sink. See Fig. 1(b) for a numerical simulation of a trajectory of Eq. (10) using the parameters from Table 1.

The basic reproductive number defined for Eq. (10) differs from the one defined for Eq. (1) in that it describes the threshold between either disease absence or disease persistence as the long term behavior. Contrasted to that, the basic reproductive defined for Eq. (1) defines the threshold for disease outbreak with long term behavior always being disease absence.

2.3 SIR Model with Births, Deaths and Vaccinations

We now modify Eq. (10) to include the effects of vaccinations. Let v be the rate of vaccination per capita. Assuming that vaccination occurs near the birth age, we immediately remove a percentage of individuals who would enter the susceptible class and place them in the recovered class. The following SIR model with births and deaths includes the effects of vaccinations.

$$\begin{aligned} \frac{dS}{dt} &= \frac{-\beta SI}{N} + (1-v)\mu N - \mu S, \\ \frac{dI}{dt} &= \frac{\beta SI}{N} - \kappa I - \mu I, \\ \frac{dR}{dt} &= \kappa I + v\mu N - \mu R. \end{aligned} \tag{19}$$

As before, the population remains constant and we do not need to consider the recovered class in our analysis. This system has two fixed points representing the DFE and the EE, with the DFE given by $(S, I) = (N(1-v), 0)$. Similar to the SIR model with births and deaths, we can linearize about the DFE. Let $dS/dt = F_1(S, I)$, $dI/dt = F_2(S, I)$ and $\mathbf{F} = \langle F_1, F_2 \rangle$. The Jacobian of $\mathbf{F}$ is

$$J_{\mathbf{F}} = \begin{bmatrix} -\frac{\beta I}{N} - \mu & -\frac{\beta S}{N} \\ \frac{\beta I}{N} & \frac{\beta S}{N} - \kappa - \mu \end{bmatrix}. \tag{20}$$

The Jacobian evaluated at $(N(1-v), 0)$ is

$$J_{\mathbf{F}}|_{(N(1-v),0)} = \begin{bmatrix} -\mu & -\beta(1-v), \\ 0 & \beta(1-v) - \kappa - \mu \end{bmatrix}, \tag{21}$$

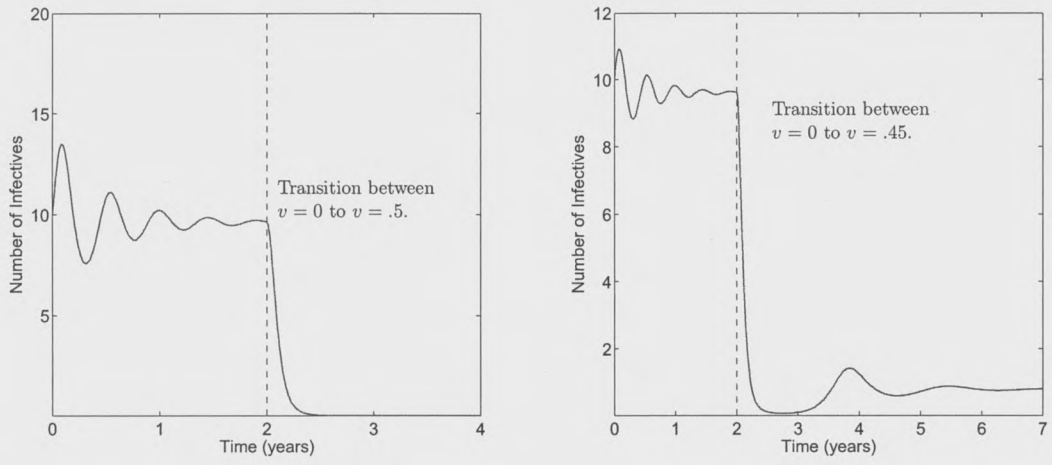

Figure 2: Numerical Simulations of the SIR model with births, deaths, and vaccinations. The dotted line in (a) shows the transition to vaccinating at a rate sufficient to ensure $R_0 < 1$. We see the solution converging to the DFE. The dotted line in (b) shows the transition to vaccinating at an *insufficient* rate leaving $R_0 > 1$. Here we see the number of infectives converging to non-zero solution.

with eigenvalues

$$\begin{aligned} \lambda_1 &= -\mu, \\ \lambda_2 &= \beta(1-v) - \kappa - \mu. \end{aligned} \tag{22}$$

The fixed point $(S, I) = (N(1-v), 0)$ representing the DFE is locally stable when

$$\beta(1-v)/(\kappa+\mu) < 1$$

and unstable when $\beta(1-v)/(\kappa+\mu) > 1$. We define $R_0 = \beta(1-v)/(\kappa+\mu)$. If $R_0 > 1$, then the fixed point

$$(\tilde{S}, \tilde{I}) = \left(\frac{N(\kappa+\mu)}{\beta}, \frac{\mu N[\beta(1-v) - \mu - \kappa]}{\beta(\kappa+\mu)} \right) \tag{23}$$

becomes locally stable.

Vaccinating provides a way to have some control over disease dynamics. A particular disease may have an unstable DFE, and therefore vaccinations can reduce $R_0 < 1$. We can examine this scenario by looking at a time series of infectives in which a fixed vaccination rate is incorporated after a certain time. We use the parameter values from Table 1. See Fig. 2(a) for a time series displaying the effect of a vaccination rate v such that $R_0 < 1$. Even if the maximum attainable vaccination rate can not reduce the value of R_0 below one, it can still have advantageous quantitative effects on the number of infected individuals as seen in Fig. 2(b).

3 Coupled Models

We use the term coupled to describe how individuals from two or more populations mix with one another. There are two types of coupling that will be used in the following model: linear migration and mass action mixing. Linear migration is defined as the event in which an individual permanently moves from one population to another. The rate is given by individuals per unit time. Mass action mixing is defined as the event when an individual temporarily moves to another population but eventually returns to their home population.

The motivation of coupling two single population models is based in capturing vital disease dynamics of measles between the northern and southern regions of Cameroon. Much work has been done to consider the effects on disease dynamics caused by mass action mixing [5]. In a more recent work, the importance of linear migration was established motivating our work to consider the relationship between both types of coupling [7].

3.1 Full Cameroon Model

The following model considers two single population models given by Eq. (19) linked by mass action mixing and linear migration. Let S_k, I_k, and R_k denote the disease classes, μ_k denote the birth/death rates, and v_k denote the vaccination rates of population N_k for $k = 1, 2$. To model linear migration, let c_1 denote the rate of migration from population two to population one and vice versa for the rate c_2. Mass action mixing will be modeled as a scaling of the number of infectives from one population who temporarily move into the second population and mix with the susceptibles to produce additional infections per unit time. We will let c_3 represent the scaling value of the infectives for the mass action mixing.

$$\begin{aligned}
\frac{dS_1}{dt} &= \frac{-\beta S_1 I_1}{N_1} - c_3\frac{\beta S_1 I_2}{N_1} + (1-v_1)\mu_1 N_1 - \mu_1 S_1 + c_1 S_2 - c_2 S_1,\\
\frac{dI_1}{dt} &= \frac{\beta S_1 I_1}{N_1} + c_3\frac{\beta S_1 I_2}{N_1} - \mu_1 I_1 - \kappa I_1 + c_1 I_2 - c_2 I_1,\\
\frac{dR_1}{dt} &= \kappa I_1 - \mu_1 R_1 + v_1\mu_1 N_1 + c_1 R_2 - c_2 R_1,\\
\frac{dS_2}{dt} &= \frac{-\beta S_2 I_2}{N_2} - c_3\frac{\beta S_2 I_1}{N_2} + (1-v_2)\mu_2 N_2 - \mu_2 S_2 + c_2 S_1 - c_1 S_2,\\
\frac{dI_2}{dt} &= \frac{\beta S_2 I_2}{N_2} + c_3\frac{\beta S_2 I_1}{N_2} - \mu_2 I_2 - \kappa I_2 + c_2 I_1 - c_1 I_2,\\
\frac{dR_2}{dt} &= \kappa I_2 - \mu_2 R_2 + v_2\mu_2 N_2 + c_2 R_1 - c_1 R_2.
\end{aligned} \tag{24}$$

We have allowed for different birth/death and vaccination rates while we kept the contact and recovery rates the same. Based on demographical research, the contact rates are approximately the same whereas the birth/death rates have been found to be different for the northern and southern regions [2]. The recovery rate is a parameter that is derived from the biological characteristics of measles only and is minimally dependent upon demographics. The vaccination rates are different to allow for the possibility that the northern and southern regions vaccinate at different rates. The parameter values used for this model can be found in Table 2.

Table 2: Parameter Values for Full Cameroon Model

Parameter	Value	Unit	Description
N_1	4451000	people	Population size
N_2	10212000	people	Population size
ρ	2.2943	none	Ratio of N_2/N_1
β	700	year^{-1}	Contact rate
κ	100	year^{-1}	Recovery rate
μ_1	.0428	year^{-1}	Birth and death rate of N_1
μ_2	.0329	year^{-1}	Birth and death rate N_2
v_1	$[0, 1]$	per capita	Vaccination rate of N_1
v_2	$[0, 1]$	per capita	Vaccination rate of N_2
c_1	$[0, 0.1]$	year^{-1}	Linear migration rate
c_3	$[0, 0.3]$	none	Scale of mass action mixing

If we add the time derivatives for population one only, (that is $dS_1/dt + dI_1/dt + dR_1/dt$) and cancel like terms, we are left with a collection of terms whose sum is not necessarily equal to zero. If we set the sum of these terms to zero, then population one will remain constant and consequently, population two will remain constant. Since this will greatly aid in the analysis we set this collection equal to zero and simplify.

$$\begin{aligned} c_2(S_1 + I_1 + R_1) - c_1(S_2 + I_2 + R_2) &= 0 \implies \\ c_2 N_1 - c_1 N_2 &= 0 \implies \\ c_2 &= c_1 N_2 / N_1. \end{aligned} \tag{25}$$

Let $\rho = N_2/N_1$ so that $c_2 = c_1\rho$. This relationship keeps both populations constant and therefore we do not need to consider both recovered classes in our analysis.

3.2 DFE Analysis with Symmetric Vaccination (SV)

We are interested in the stability of the fixed points of Eq. (24). Until otherwise specified, we assume the vaccination rates are symmetric so that $v_1 = v_2 = v$. Although this is a stronger condition, as an initial step, it will greatly reduce the complexity of the analysis and will also lead to an important fact about vaccinating at symmetric rates.

There are two fixed points of Eq. (24) that represent the two familiar distinct disease states: the DFE and the EE. For the remainder of the paper, we will focus solely on the stability of the DFE. The DFE is given by

$$(\tilde{S}_1, \tilde{I}_1, \tilde{S}_2, \tilde{I}_2) = (N_1(1-v), 0, -N_1\rho(v-1), 0). \tag{26}$$

As before, we let $dS_1/dt = F_1(S_1, I_1, S_2, I_2)$, $dI_1/dt = F_2(S_1, I_1, S_2, I_2)$, $dS_2/dt = F_3(S_2, I_2, S_2, I_2)$, $dI_2/dt = F_4(S_2, I_2, S_2, I_2)$, and $\mathbf{F} = \langle F_1, F_2, F_3, F_4 \rangle$. The Jacobian of $\mathbf{F}$ is

$$J_{\mathbf{F}} = \begin{bmatrix} J_1 & J_2 \\ J_3 & J_4 \end{bmatrix}, \tag{27}$$

where

$$J_1 = \begin{bmatrix} -\dfrac{\beta(I_1 + c_3 I_2)}{N_1} - \mu_1 - c_1\rho & -\dfrac{\beta S_1}{N_1} \\ \dfrac{\beta(I_1 + c_3 I_2)}{N_1} & \dfrac{\beta S_1}{N_1} - \kappa - \mu_1 - c_1\rho \end{bmatrix}, \quad J_2 = \begin{bmatrix} c_1 & -\dfrac{c_3\beta S_1}{N_1} \\ 0 & \dfrac{c_3\beta S_1}{N_1} + c_1 \end{bmatrix},$$

$$J_3 = \begin{bmatrix} c_1\rho & -\dfrac{c_3\beta S_2}{\rho N_1} \\ 0 & \dfrac{c_3\beta S_2}{\rho N_1} + c_1\rho \end{bmatrix}, \quad J_4 = \begin{bmatrix} -\dfrac{\beta(I_2 + c_3 I_1)}{\rho N_1} - \mu_2 - c_1 & -\dfrac{\beta S_2}{\rho N_1} \\ \dfrac{\beta(I_2 + c_3 I_1)}{\rho N_1} & \dfrac{\beta S_2}{\rho N_1} - \kappa - \mu_2 - c_1 \end{bmatrix}.$$

The Jacobian of $\mathbf{F}$ evaluated at $(\tilde{S}_1, \tilde{I}_1, \tilde{S}_2, \tilde{I}_2)$ is $J_{\mathbf{F}}|_{(\tilde{S}_1, \tilde{I}_1, \tilde{S}_2, \tilde{I}_2)} =$

$$\begin{bmatrix} -(\mu_1 + c_1\rho) & -\beta(1-v) & c_1 & -c_3\beta(1-v) \\ 0 & \beta(1-v) - \kappa - \mu - c_1\rho & 0 & c_3\beta(1-v) + c_1 \\ c_1\rho & -c_3\beta(1-v) & -(\mu_2 + c_1) & -\beta(1-v) \\ 0 & c_3\beta(1-v) + c_1\rho & 0 & \beta(1-v) - \kappa - \mu_2 - c_1 \end{bmatrix},$$

with eigenvalues

$$\begin{aligned}
\lambda_1 &= -\frac{1}{2}\left(c_1(\rho+1)+\mu_1+\mu_2-\sqrt{(c_1(1+\rho)+\mu_1-\mu_2)^2-4c_1(\mu_1-\mu_2)}\right),\\
\lambda_2 &= -\frac{1}{2}\left(c_1(\rho+1)+\mu_1+\mu_2+\sqrt{(c_1(1+\rho)+\mu_1-\mu_2)^2-4c_1(\mu_1-\mu_2)}\right),\\
\lambda_3 &= \beta(1-v)-\kappa-\frac{1}{2}(c_1(1+\rho)+\mu_2+\mu_1)\\
&+\frac{1}{2}\sqrt{(c_1(\rho+1)+\mu_1-\mu_2)^2-4c_1(\mu_1-\mu_2)+4c_3\beta(1-v)(c_3\beta(1-v)+c_1(\rho+1))},\\
\lambda_4 &= \beta(1-v)-\kappa-\frac{1}{2}(c_1(\rho+1)+\mu_2+\mu_1)\\
&-\frac{1}{2}\sqrt{(c_1(\rho+1)+\mu_1-\mu_2)^2-4c_1(\mu_1-\mu_2)+4c_3\beta(1-v)(c_3\beta(1-v)+c_1(\rho+1))}.
\end{aligned}$$

The DFE is stable when all the eigenvalues have negative real parts. To analyze the eigenvalues, we first consider the various cases in which one type of coupling is absent. We want to examine how the vaccination rate needed for a stable DFE is affected by only that type of coupling.

3.2.1 Basic Reproductive Number: Linear Migration Only

We let $c_3 = 0$ for this section and analyze the effect linear migration has on the stability of the DFE. In this case, the eigenvalues of Eq. (24) reduce to

$$\begin{aligned}
\lambda_1 &= -\tfrac{1}{2}\left(c_1(\rho+1)+\mu_1+\mu_2-\sqrt{(c_1(\rho+1)+\mu_1-\mu_2)^2-4c_1(\mu_1-\mu_2)}\right),\\
\lambda_2 &= -\tfrac{1}{2}\left(c_1(\rho+1)+\mu_1+\mu_2+\sqrt{(c_1(\rho+1)+\mu_1-\mu_2)^2-4c_1(\mu_1-\mu_2)}\right),\\
\lambda_3 &= \beta(1-v)-\kappa+\lambda_1,\\
\lambda_4 &= \beta(1-v)-\kappa+\lambda_2.
\end{aligned} \tag{28}$$

In order to define the basic reproductive number for this case, we need to analyze the real parts of the eigenvalues in Eq. (28). First, let

$$\begin{aligned}
\theta_1 &= c_1(\rho+1)+\mu_1+\mu_2,\\
\theta_2 &= (c_1(\rho+1)+\mu_1-\mu_2)^2-4c_1(\mu_1-\mu_2).
\end{aligned} \tag{29}$$

If we consider θ_2 as a quadratic expression in c_1 with leading coefficient $(\rho+1)^2$, it attains an absolute minimum at $d\theta_2/dc_1 = 0$. Solving this equation gives $c_1 = \frac{\mu_1-\mu_2}{(\rho+1)^2}$. Substituting this expression into θ_2 to find the absolute minimum gives

$$\frac{4\rho(\mu_1-\mu_2)^2}{(\rho+1)^2}, \tag{30}$$

which is clearly positive. Hence, $\theta_2 > 0$, and all the eigenvalues are real valued. Upon inspection we see that $\theta_1 > 0$ and therefore $\lambda_2 < 0$. In considering λ_1, if $\theta_1 > \sqrt{\theta_2}$, then $\lambda_1 < 0$. Simplifying $\theta_1 > \sqrt{\theta_2}$ yields $c_1 > \dfrac{-\mu_1\mu_2}{\mu_\rho + 1\mu_2}$. Since $c_1 > 0 > \dfrac{-\mu_1\mu_2}{\mu_\rho + 1\mu_2}$ is always true, then $\lambda_1 < 0$.

Since $\theta_1, \theta_2 > 0$, then $\theta_1 + \sqrt{\theta_2} > \theta_1 - \sqrt{\theta_2} \implies -\frac{1}{2}(\theta_1 + \sqrt{\theta_2}) < -\frac{1}{2}(\theta_1 - \sqrt{\theta_2})$ and so $\lambda_2 < \lambda_1$. Therefore, for $\theta_3 = \beta(1-v) - \kappa$,

$$\begin{aligned} \lambda_3 &= \theta_3 + \lambda_1, \\ \lambda_4 &= \theta_3 + \lambda_2, \end{aligned} \tag{31}$$

it is clear that since $\lambda_3 > \lambda_4$ and $\lambda_1, \lambda_2 < 0$ for all parameter values, then λ_3 dictates the stability of the DFE. For $\lambda_3 = \beta(1-v) - \kappa + \lambda_1$, we see that $\lambda_3 < 0$ when $\beta(1-v) < \kappa - \lambda_1$. Thus $\lambda_3 < 0$ implies $\dfrac{\beta(1-v)}{\kappa - \lambda_1} < 1$. Define

$$R_{0_1} = \frac{\beta(1-v)}{\kappa - \lambda_1}. \tag{32}$$

We interpret R_{0_1} as the threshold value that describes the threshold between disease absence and persistence in both populations when $v_1 = v_2 = v$ and $c_3 = 0$. Based on this definition, R_{0_1} depends on β, κ, c_1, ρ, and v. We see that a bifurcation occurs when $R_{0_1} = 1$. Suppose $c_1 = 0$. Then the eigenvalues in Eq. (28) reduce to

$$\begin{aligned} \lambda_1 &= -\mu_2, \\ \lambda_2 &= -\mu_1, \\ \lambda_3 &= \beta(1-v) - \kappa - \mu_1, \\ \lambda_4 &= \beta(1-v) - \kappa - \mu_2. \end{aligned} \tag{33}$$

These are the eigenvalues of the uncoupled system, i.e. when $c_1 = c_3 = 0$ with λ_4 being the dominant eigenvalue. We fix the parameters in λ_4 using the values from Table 2, and solve for the value of v, say $\tilde{v}$ to ensure $R_{0_1} = 1$ when $c_1 = c_3 = 0$. We are interested in seeing the effect linear migration has on the stability of the DFE. We let c_1 vary within the interval $[0, 0.1]$ and examine the change to R_{0_1}. Figure 3(a) shows the effect linear migration has on the value of R_{0_1}. We see that increasing linear migration lowers the value of R_{0_1} thus reducing the vaccination rate needed for DFE stability. However, the effect is very minimal. We recall the assumption that both the northern and southern regions are vaccinating at the rate $\tilde{v}$. We conclude that linear migration contributes very little to the stability of the DFE when vaccination rates are *symmetric* between the populations.

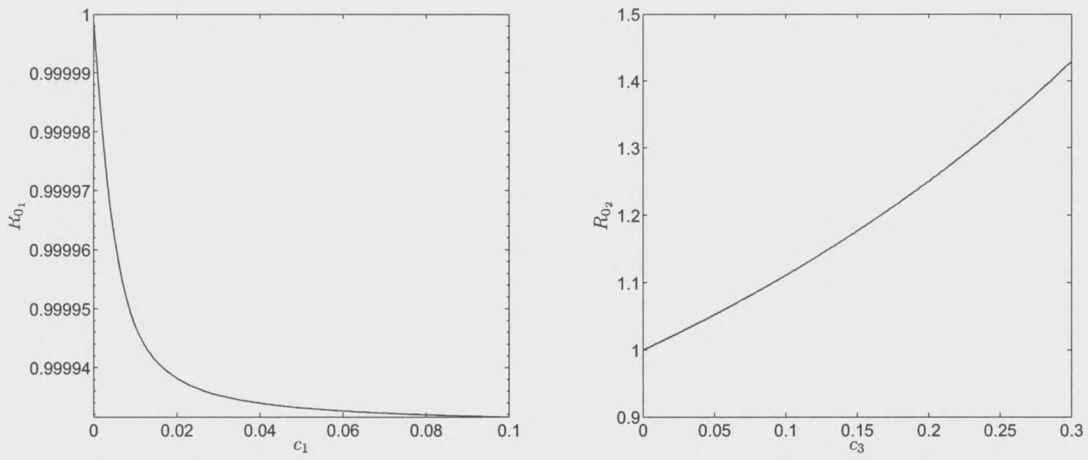

Figure 3: (a) The value of R_{0_1} as linear migration is increased with $\tilde{v} = .8575$, $c_3 = 0$ and remaining parameter values given in Table 2. (b) The value of R_{0_2} as mass action mixing is increased with $\tilde{v} = .8575$, $c_1 = 0$ and remaining parameter values given in Table 2.

3.2.2 Basic Reproductive Number: Mass Action Mixing Only

We let $c_1 = 0$ for this section and analyze the effect mass action mixing has on the stability of the DFE. In this case, the eigenvalues of Eq. (24) reduce to

$$\begin{aligned}
\lambda_1 &= -\mu_2, \\
\lambda_2 &= -\mu_1, \\
\lambda_3 &= \beta(1-v) - \kappa - \tfrac{1}{2}\left(\mu_1 + \mu_2 - \sqrt{4\beta^2 c_3^2 (1-v)^2 + (\mu_1 - \mu_2)^2}\right), \\
\lambda_4 &= \beta(1-v) - \kappa - \tfrac{1}{2}\left(\mu_1 + \mu_2 + \sqrt{4\beta^2 c_3^2 (1-v)^2 + (\mu_1 - \mu_2)^2}\right).
\end{aligned} \tag{34}$$

In order to define the basic reproductive number in this case, we must analyze the real parts of the eigenvalues in Eq. (34). Clearly, λ_1 and λ_2 are negative. Note that the expression under the common radical is the sum of two positive quantities and therefore is positive. Hence, λ_3 and λ_4 are real valued. To simplify notation, we set

$$\theta_3 = \sqrt{4\beta^2 c_3^2 (1-v)^2 + (\mu_2 - \mu_1)^2}. \tag{35}$$

Upon inspection, it is clear that $\lambda_3 > \lambda_4$. Similar to the case with linear migration, $\lambda_3 > \lambda_4$ and $\lambda_1, \lambda_2 < 0$ for all parameter values. Therefore λ_3 dictates the stability of the DFE. We see that $\lambda_3 < 0$ when $\beta(1-v) - \kappa - \frac{1}{2}(\mu_1 + \mu_2 - \theta_3) < 0$. We define

$$R_{0_2} = \frac{\beta(1-v)}{\kappa + \frac{1}{2}(\mu_2 + \mu_1 - \theta_3)} \tag{36}$$

as the basic reproductive number for Eq. (24) when $c_1 = 0$ and $v_1 = v_2 = v$. Similar to before, R_{0_2} is interpreted as the value that describes the threshold between disease absence and persistence in both populations.

Similar to before, we are interested in the effect mass action mixing has on the stability of the DFE. We let c_3 vary within the interval $[0, 0.3]$ and examine the change to R_{0_2} where $\tilde{v}$ is defined as before. Figure 3(b) shows the effect mass action mixing has on the value of R_{0_2}. We see that the stability of the DFE is much more sensitive to the value of c_3. However, we must consider the assumption that accompanies mass action mixing. Namely, that the infectives from one population who are mixing with the susceptibles are doing so in a spatially uniform sense. In a country such as Cameroon, we would expect that short term movement takes place largely at the border between the Northern and Southern regions. Therefore, we do not expect larger values of c_3 to be realistic within this model.

3.3 DFE Analysis with Non-symmetric Vaccination (NSV)

Up to this point, we have results that describe how coupling affects the vaccination rate needed to ensure that the DFE is locally stable. We concluded that linear migration has a very minimal effect on the stability under the assumption that the vaccination rate was symmetric. We now analyze the case when vaccination is non-symmetric, i.e. $v_1 \neq v_2$. We explore the possibility that coupling causes different qualitative effects on the stability of the DFE when vaccination is non-symmetric.

We begin by solving for the fixed point representing the DFE of Eq. (24). This point is given by

$$(\hat{S}_1, \hat{I}_1, \hat{S}_2, \hat{I}_2) = (N_1(1-\delta_1), 0, N_1\rho(1-\delta_2), 0), \tag{37}$$

where

$$\delta_1 = \frac{\mu_2\rho v_2 c_1 + \mu_2\mu_1 v_1 + \mu_1 v_1 c_1}{\mu_2\mu_1 + \mu_2 c_1\rho + \mu_1 c_1}, \quad \delta_2 = \frac{\mu_2\rho v_2 c_1 + \mu_2\mu_1 v_2 + \mu_1 v_1 c_1}{\mu_2\mu_1 + \mu_2 c_1\rho + \mu_1 c_1}. \tag{38}$$

In order to characterize the stability of the DFE when c_1 and c_3 are not both zero, we evaluate the Jacobian of Eq. (24) at $(\hat{S}_1, \hat{I}_1, \hat{S}_2, \hat{I}_2)$ and seek out the dominant eigenvalue. The first two eigenvalues are identical to λ_1 and λ_2 in Eq. (28) which have been shown to be negative. The other two eigenvalues, λ_3 and λ_4 are conjugate pairs given by

$$\lambda_3 = -\frac{1}{2}(a - \sqrt{b}), \quad \lambda_4 = -\frac{1}{2}(a + \sqrt{b}). \tag{39}$$

The expressions a and b are given below:

$$\begin{aligned} a &= c_1(\rho+1) + \mu_1 + \mu_2 + \beta(\delta_2 + \delta_1 - 2) + 2\kappa, \\ b &= 4(1-\delta_2)(1-\delta_1){c_3}^2\beta^2 + (\beta(\delta_1-\delta_2) + \mu_1 - \mu_2)^2 + \\ &\quad (\rho+1)^2{c_1}^2 + 2c_1(\rho-1)(\mu_1-\mu_2) + \beta(4(1-\delta_1)c_3c_1\rho + \\ &\quad 4(1-\delta_2)c_3c_1 + 2c_1(\rho-1)(\delta_1-\delta_2)). \end{aligned}$$

We see $0 \leq \delta_i \leq 1$ for $i = 1, 2$ because $0 \leq v_1, v_2 \leq 1$. Thus $(1 - \delta_i) \geq 0$ for $i = 1, 2$. If we assume $v_1 \geq v_2$, then by inspection all the terms are positive in

b with parameter values given in Table 2. Otherwise, the expression b must be checked for the parameters of interest. Therefore, if $b \geq 0$, then λ_3 and λ_4 are real-valued, and the sign of λ_3 determines the stability of the DFE.

We are interested in the relationship between the vaccination rates. Fixing all parameter values except v_1 and v_2, we set $\lambda_3 = 0$ and solve for the non-spurious function $v_2 = f(v_1)$ to give the relationship describing the bifurcation points of the DFE. Because this relationship depends on the coupling, various values for c_1 and c_3 are considered. These changes to the coupling will allow us to examine how the bifurcations of the DFE are affected. Refer to Fig. 4(a-d).

Each of these figures display the bifurcation points of the DFE for various values of c_1 and c_3. The black dotted lines represent the uncoupled vaccination rates needed to ensure the DFE is stable in each population. These rates were computed using the eigenvalues in Eq. (33). They are a reference that allows us to examine how coupling effect the vaccination rates needed for stability.

For each point in the (v_1, v_2) space and fixed coupling parameters, if $v_2 > f(v_1)$ then the point (v_1, v_2) will be located in a stable region and the disease will die out. Otherwise, if $v_2 < f(v_1)$, then the point (v_1, v_2) is located in an unstable region and the disease will persist. From these diagrams it is clear that increasing the linear migration rate c_1 enlarges the region of stability for a specified mass action coupling rate c_3. However, as c_3 is increased the region of stability reduces. We can see this distinction when we compare Fig. 4(a) and 5(b).

These figures also give us a graphical verification of the fact stated earlier; that linear migration has a very minimal effect on the stability of the DFE when vaccination is symmetric. The line $v_2 = v_1$ in the parameter space (v_1, v_2) intersects the curves describing the bifurcation points at approximately the same point. This point is on each of the curves generated with different values of c_1 thus verifying that stability of the DFE is essentially independent of the value of c_1 for symmetric vaccination.

4 Numerical Analysis and Verification

Numerically solving Eq. (24) can help us determine important quantitative information about the system that would otherwise be too analytically complex to derive. For example, finding the fixed point representing the EE of Eq. (24) is algebraically intractable and therefore can not be easily manipulated. However, the EE can be found numerically using specified parameter values. In this section we will compute the EE, as well as verify the results established thus far. Before continuing though we note that due to the very small magnitudes that arise in the coupled system, the ode45 solver loses accuracy. For example, when I_1 asymptotically approaches zero, values approach machine precision causing numerical error. We must first transform Eq. (24) using a change of variables to avoid this problem.

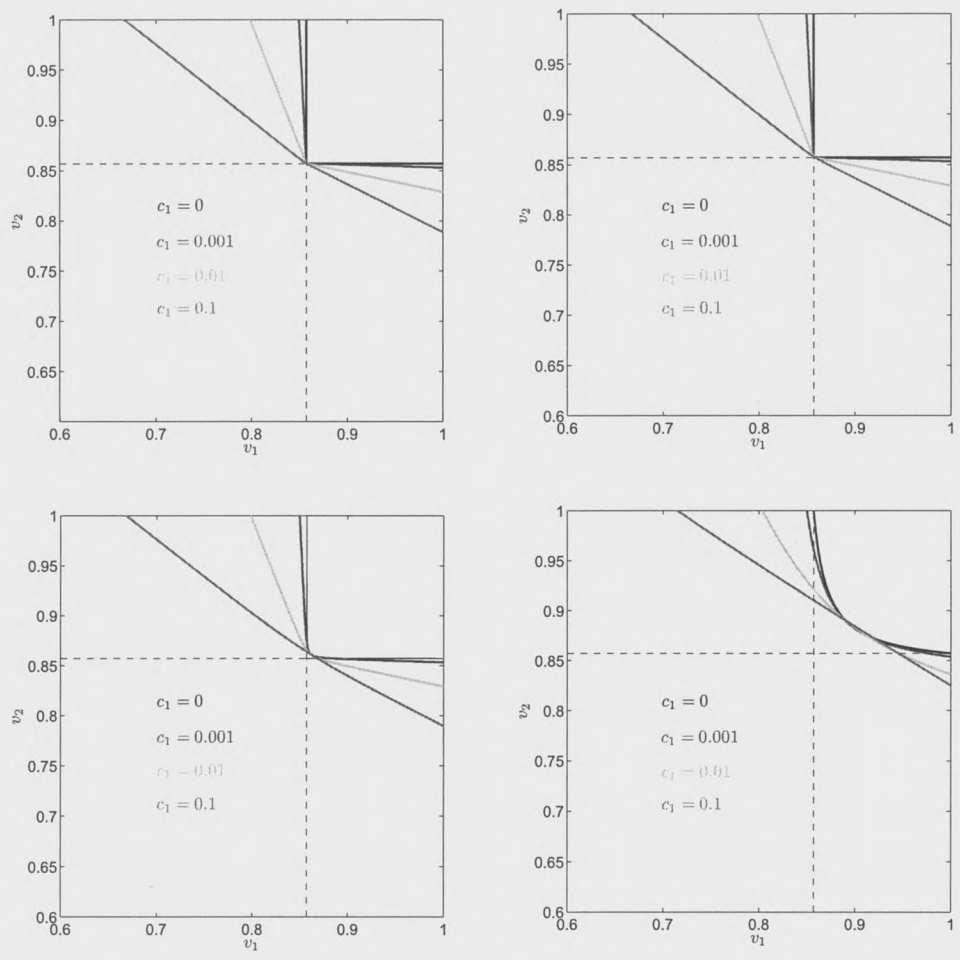

Figure 4: Plots of $v_2 = f(v_1)$ describing the bifurcation points of the DFE with varying values of c_1. Parameter are given by the values in Table 2. The mass action rate was varied for each of the figure with (a) $c_3 = 0$, (b) $c_3 = 0.003$, (c) $c_3 = 0.03$, (d) $c_3 = 0.3$.

4.1 Full Cameroon Model: Change of Variables

We perform a change of variables to the Eq. (24) with the prior substitution $c_2 = c_1\rho$ to deal with the numerical error that would arise from using the original system. First, ignoring the recovered classes, we normalize the populations by making the following substitutions:

$$s_k = S_k/N_k, \quad i_k = I_k/N_k, \tag{40}$$

for $k = 1, 2$. Next,

$$\frac{ds_k}{dt} = \frac{1}{N_k}\frac{dS_k}{dt}, \quad \frac{di_k}{dt} = \frac{1}{N_k}\frac{dI_k}{dt}, \tag{41}$$

for $k = 1, 2$. Note that this normalization restricts our domain to the interval $[0, 1]$ for each class. We then use the following logarithmic change of variables:

$$x_k = \ln s_k, \quad y_k = \ln i_k, \tag{42}$$

for $k = 1, 2$. This change of variable essentially 'stretches' the domain thereby allowing for accurate computation. Note though that the domain for each disease class is $[0, 1]$ which must be restricted to $(0, 1]$ so that the logarithmic change of variables is well defined. By the chain rule,

$$\frac{dx_k}{dt} = \frac{1}{s_k}\frac{ds_k}{dt}, \quad \frac{dy_k}{dt} = \frac{1}{i_k}\frac{di_k}{dt}. \tag{43}$$

The resulting sytem is

$$\begin{aligned}
\frac{dx_1}{dt} &= -\beta e^{x_2} - c_3\rho\beta e^{y_2} + (1 - v_1)\mu_1 e^{-x_1} - \mu_1 + c_1\rho e^{y_1 - x_1} - c_1\rho \\
\frac{dy_1}{dt} &= \beta e^{x_1} + c_3\rho\beta e^{x_1 + y_2 - x_2} - \kappa - \mu_1 + c_1\rho e^{y_2 - x_2} - c_1\rho \\
\frac{dy_1}{dt} &= -\beta e^{y_2} - \frac{1}{\rho}c_3\beta e^{x_2} + (1 - v_2)\mu_2 e^{-y_1} - \mu_2 + c_1 e^{x_1 - y_1} - c_1 \\
\frac{dy_2}{dt} &= \beta e^{y_1} + \frac{1}{\rho}c_3\beta e^{y_1 + x_2 - y_2} - \kappa - \mu_2 + c_1 e^{x_2 - y_2} - c_1.
\end{aligned} \tag{44}$$

4.2 Simulations and Verifications

A trajectory of the EE of Eq. (44) can be simulated using parameter values from Table 2 with $v_1 = v_2 = 0$ and non-zero coupling rates. The initial condition used is slightly perturbed off the number of infectives at the theoretical EE so that the transient behavior can be observed. Figure 5 shows a numerical simuations of a trajectory of Eq. (44). The oscillatory nature of the transients tell us that the EE is a stable spiral sink. We can see this oscillatory behavior clearly by looking at the EE for each population in the (S_k, I_k) phase plane for $k = 1, 2$.

To verify an instance where a bifurcation occurs as the linear migration rate increases, we simulate Eq. (44) for parameter values that ensure an unstable DFE. After a specified amount of time, we then increase the linear migration rate and examine the changes to the number of infected individuals. See Fig. 7(a) and (b). For these simulations, v_1 and v_2 were chosen to ensure that the DFE was unstable for $c_1 = 0$, 0.001, 0.01, but stable for $c_1 = 0.1$.

5 Stochastic Approach

The model given by Eq. (24) is deterministic. It describes the mean behavior of the quantities involved. For any initial condition in a neighborhood of the phase space, the trajectory is uniquely determined and will approach a stable steady state. These trajectories have no fluctuations due to external noise. Because noise induced phenomenon is a much more realistic interpretation of real world characteristics, it motivates us to analyze our model stochastically. This type of analysis will allow low probability events, i.e. events induced by noise, to be captured that would otherwise go unnoticed in a completely deterministic system. For example, disease

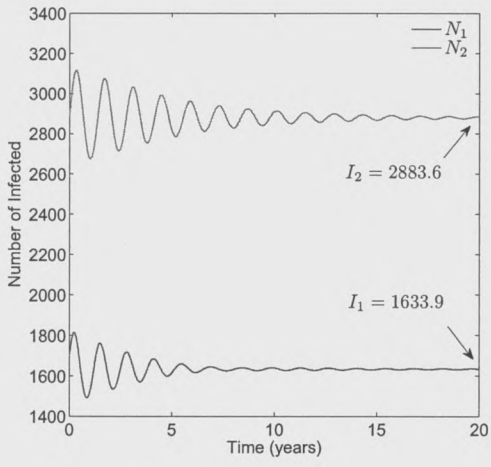

Figure 5: Numerical simulation of Eq. (44) displaying the endemic equilibrium for N_1 and N_2 with $v_1 = v_2 = 0$, $c_1 = 0.01$, $c_3 = 0.003$, and parameter values given in Table 2. The resulting solution was tranformed back to the quantities $I_1, I, 2$ representing the number of infected individuals.

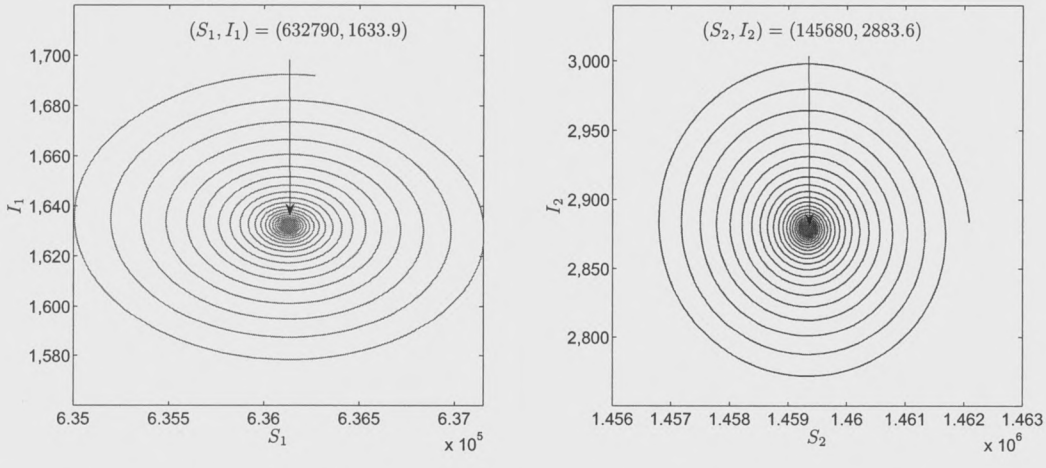

Figure 6: Trajectories showing that the EE for each population is a stable spiral sink for $v_1 = v_2 = 0$ and $c_1 = 0.01$ and $c_3 = 0.003$. The resulting solution was tranformed back to the quantities $I_1, I, 2, S_1, S_2$ representing the number of infected individuals.

fade out, i.e. the event when the disease becomes absent in the population, can not happen when the basic reproductive number is greater than one in a deterministic system. Any initial condition will be attracted to the stable EE and therefore both I_1 and I_2 will be greater than zero for all $t > 0$. Using a stochastic approach, this type of scenario is perfectly possible, and in fact, will be the type of behavior we seek out exclusively.

We see that disease fade out is captured stochastically when the fluctuations about the mean behavior cause the number of infectives to spontaneously go to zero. Because oscillations are inherent due to the EE being a spiral sink, fluctuations due

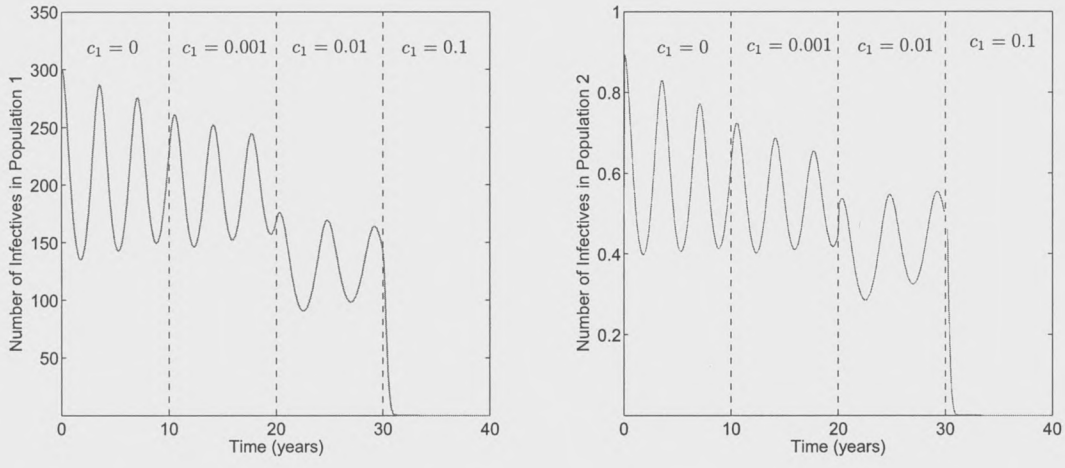

Figure 7: (a) Infectives of N_1 and (b) Infectives of N_2 as c_1 is increased from 0 to 0.1 with $v_1 = 0.75$, $v_2 = 0.94$, and $c_3 = .003$. The resulting solution was tranformed back to the quantities $I_1, I, 2$ representing the number of infected individuals.

to noise about this mean behavior will create more pronounced fluctuations. Thus allowing for the infectives to spontaneously go to zero more easily. Since vaccination is the primary way to control the number of infectives quantitatively, we seek the minimal vaccination rate to ensure a consistent fade out. We will make use of the results established thus far about non-symmetric vaccination to maximize its effect.

5.1 Stochastic Representation of Full Cameroon Model

The stochastic algorithm used for this research is based on the method described by Gillespie[3]. The algorithm is similar to a Monte Carlo process in that it uses repeated random sampling. First, a random number is used to generate a time step t. At this time step, another random number is used to select an event. An event is represented by a term within the model. For example, the term κI_1 is the event in which a person moves from the infected class to the recovered class in population one. The probability that an event is selected at some time step is its numerical value divided by the sum of the numerical values of all the events in the system. Once the event is selected, the necessary change is made to each compartment of the model corresponding to that event. This process is repeated many times to attain a stochastic time evolution of the model.

To stochastically represent the deterministic system using the Gillespie method, we must consider each distinct term in the system as a particular probabilistic event with a specific outcome. Let $\mathbf{X} = \langle S_1(t_k), I_1(t_k), R_1(t_k), S_2(t_k), I_2(t_k), R_2(t_k)\rangle$ denote the value of each class at time t_k and $\mathbf{r} = \langle r_1, r_2, r_3, r_4, r_5, r_6\rangle$ with the ordered components denoting the increments in S_1, I_1, R_1, S_2, I_2, and R_2 at time t_{k+1} respectively. Define $\mathbf{W}(\mathbf{X} : \mathbf{r})$ as the transition rate for an event. The transition

rates and their corresponding events for Eq. (24) are:

$$\mathbf{W}(\mathbf{X} : \langle 1,0,0,0,0,0\rangle) = (1-v_1)\mu_1 N_1 \qquad \text{Birth in } N_1,$$
$$\mathbf{W}(\mathbf{X} : \langle 0,0,1,0,0,0\rangle) = v_1\mu_1 N_1 \qquad \text{Vaccination in } N_1,$$
$$\mathbf{W}(\mathbf{X} : \langle -1,0,0,0,0,0\rangle) = \mu_1 S_1 \qquad \text{Death in } S_1,$$
$$\mathbf{W}(\mathbf{X} : \langle 0,-1,0,0,0,0\rangle) = \mu_1 I_1 \qquad \text{Death in } I_1,$$
$$\mathbf{W}(\mathbf{X} : \langle 0,0,-1,0,0,0\rangle) = \mu_1 R_1 \qquad \text{Death in } R_1,$$
$$\mathbf{W}(\mathbf{X} : \langle -1,1,0,0,0,0\rangle) = \tfrac{\beta S_1 I_1}{N_1} \qquad \text{Infection in } N_1,$$
$$\mathbf{W}(\mathbf{X} : \langle -1,1,0,0,0,0\rangle) = c_3\tfrac{\beta S_1 I_2}{N_1} \qquad \text{Infection in } N_1,$$
$$\mathbf{W}(\mathbf{X} : \langle 0,-1,1,0,0,0\rangle) = \kappa I_1 \qquad \text{Recovery in } N_1,$$
$$\mathbf{W}(\mathbf{X} : \langle 1,0,0,-1,0,0\rangle) = c_1 S_2 \qquad \text{Migration of susceptible from } N_2 \text{ to } N_1,$$
$$\mathbf{W}(\mathbf{X} : \langle 0,1,0,0,-1,0\rangle) = c_1 I_2 \qquad \text{Migration of infective from } N_2 \text{ to } N_1,$$
$$\mathbf{W}(\mathbf{X} : \langle 0,0,1,0,0,-1\rangle) = c_1 R_2 \qquad \text{Migration of recovered from } N_2 \text{ to } N_1,$$
$$\mathbf{W}(\mathbf{X} : \langle 0,0,0,1,0,0\rangle) = (1-v_2)\mu_2 N_2 \qquad \text{Birth in } N_2,$$
$$\mathbf{W}(\mathbf{X} : \langle 0,0,0,0,0,1\rangle) = v_2\mu_2 N_2 \qquad \text{Vaccination in } N_2,$$
$$\mathbf{W}(\mathbf{X} : \langle 0,0,0,-1,0,0\rangle) = \mu_2 S_2 \qquad \text{Death in } S_2,$$
$$\mathbf{W}(\mathbf{X} : \langle 0,0,0,0,-1,0\rangle) = \mu_2 I_2 \qquad \text{Death in } I_2,$$
$$\mathbf{W}(\mathbf{X} : \langle 0,0,0,0,0,-1\rangle) = \mu_2 R_2 \qquad \text{Death in } R_2,$$
$$\mathbf{W}(\mathbf{X} : \langle 0,0,0,-1,1,0\rangle) = \tfrac{\beta S_2 I_2}{\rho N_1} \qquad \text{Infection in } N_2,$$
$$\mathbf{W}(\mathbf{X} : \langle 0,0,0,-1,1,0\rangle) = c_3\tfrac{\beta S_2 I_1}{\rho N_1} \qquad \text{Infection in} N_2,$$
$$\mathbf{W}(\mathbf{X} : \langle 0,0,0,0,-1,1\rangle) = \kappa I_2 \qquad \text{Recovery in } N_2,$$
$$\mathbf{W}(\mathbf{X} : \langle 1,0,0,-1,0,0\rangle) = c_1\rho S_1 \qquad \text{Migration of susceptible from } N_1 \text{ to } N_2,$$
$$\mathbf{W}(\mathbf{X} : \langle 0,1,0,0,-1,0\rangle) = c_1\rho I_1 \qquad \text{Migration of infective from } N_1 \text{ to } N_2,$$
$$\mathbf{W}(\mathbf{X} : \langle 0,0,1,0,0,-1\rangle) = c_1\rho R_1 \qquad \text{Migration of recovered from } N_1 \text{ to } N_2.$$

The next time step t_{k+1} is computed by the expression

$$t_{k+1} = t_k + \tau \tag{45}$$

where

$$\tau = \frac{1}{a_0}\ln\left(\frac{1}{r_1}\right), \tag{46}$$

and a_0 is the sum of all the numerical values of all the events at time t_k, and r_1 is a randomly generated number in the interval $[0,1]$. We note that τ is using the same distribution. Initially, $t_0 = 0$ and

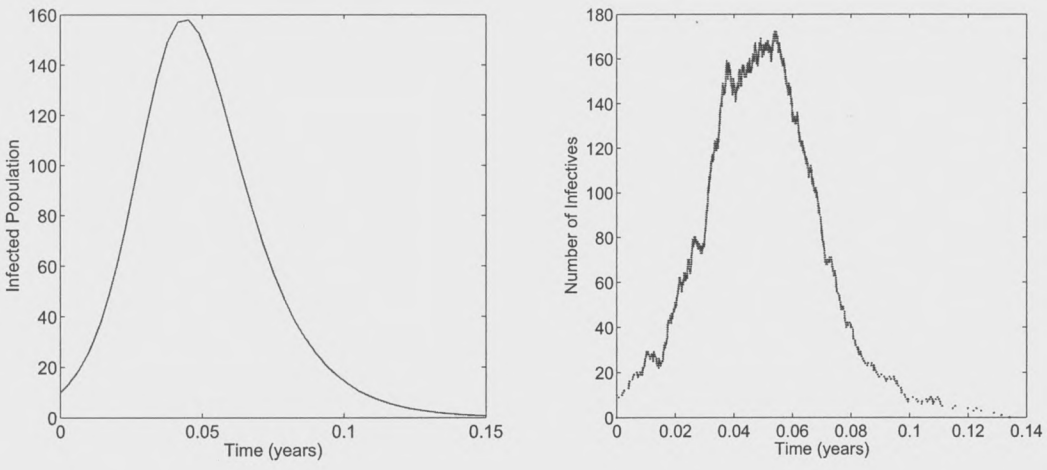

Figure 8: Deterministic and stochastic trajectories of Eq. (1) with parameters given by the values in Table 1.

$\langle S_1(t_0), I_1(t_0), R_1(t_0), S_2(t_0), I_2(t_0), R_2(t_0)\rangle = \langle S_1(0), I_1(0), R_1(0), S_2(0), I_2(0), R_2(0)\rangle$. It is important to note that this discrete time step in not uniform since the step size is inversely related to a_0. Hence, smaller time steps are created as the event's numerical values increase resulting in greater frequency of repeated samples.

An actual event is selected at t_k by first generating a second random number r_2 in the interval $[0, 1]$. The product $a_0 r_2$ can therefore be thought of as some random location on the interval $[0, a_0]$. If the order of the values of the events are kept track of, then $a_0 r_2$ 'falls' onto precisely one subinterval of $[0, a_0]$ corresponding to exactly one event. Since the event is known, its transition rate is applied to $\mathbf{X}$ and t_{k+1} is generated. This process is then repeated a large number of times. For the remainder of the paper, we will refer to the stochastic representation of Eq. (24) as the Full Stochastic Model (FSM) using parameter values given in Table 2 for all simulations.

5.2 Stochastic Simulations and Verifications

To visual the effect between deterministic and stochastic solutions, we can use the Gillespie algorithm to simulate trajectories of basic models. Using Eq. (1) as an example, we simulate the deterministic and stochastic time series with the same initial condition and parameters in Fig. 8(a) and 8(b). It is easy to identify fluctuations about the mean behavior in these figures. We can also see fadeout occurring in the stochastic simulation, whereas the number of infectives in the deterministic simulation asymptotically approach zero.

A simulation of the FSM can be seen in Fig. 9(a). The number of infectives at the initial condition is set to the exact values at the EE. The pronounced oscillatory behavior is a result of the mean oscillatory behavior in the deterministic time series. The large fluctuations bring the number of infectives to very low values in some instances, which is precisely the behavior that we are looking to capture as we

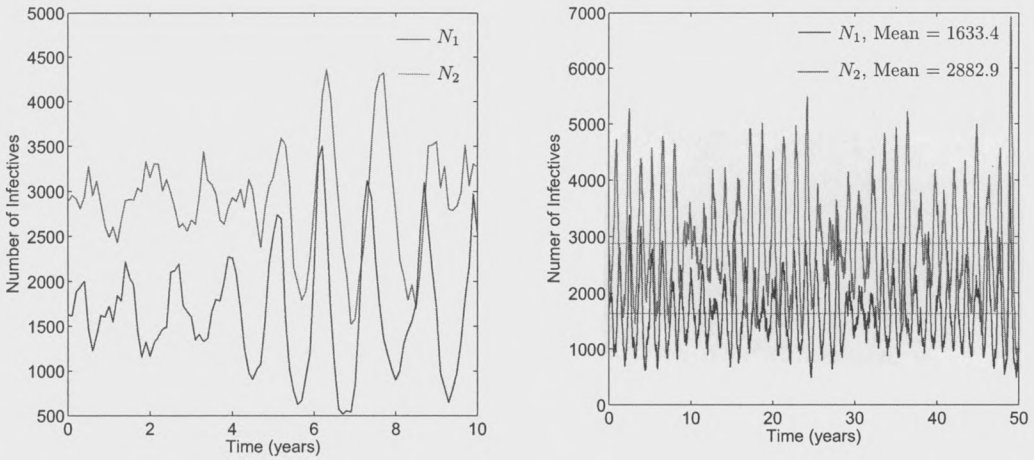

Figure 9: (a) Stochastic simulation of the FSM with $c_1 = 0.01$, $c_3 = 0.003$, and $v_1 = v_2 = 0$. (b) Average number of infectives in each population computed from the stochastic simulation for a fifty year interval.

increase the vaccination rates.

Because the Gillespie algorithm uses repeated sampling, verifying the mean behavior stochastically requires us to average the long term endemic behavior for a sufficient time. In Fig. 9(b), the average number of infectives is computed and displayed. The mean values derived from the stochastic simulation are nearly identical to the deterministic values verifying that the stochastic simulation does indeed oscillate around the deterministic mean with some distribution. It is also worth noting that we do *not* see any convergent behavior toward the EE. In fact, regardless of the number of time steps used in a single simulation, convergence will not be observed.

5.3 Stochastic Analysis of Fadeout with NSV

As described before, fadeout is the event when the number of infectives spontaneously go to zero. We have already demonstrated that large fluctuations about the mean occur in the FSM. Since nonzero vaccination rates lower the value of the deterministic mean, then the fluctuations observed in simulations of the FSM should lead to fadeout. In Fig. 4, we have already established the bifurcation points in the (v_1, v_2) of the deterministic system. Certainly, using any (v_1, v_2) describing a bifurcation point will lead to fadeout. What is of interest now is to establish how much (v_1, v_2) can be lowered so that fadeout occurs consistently in a small interval of time. We expect that there is a certain threshold in which the disease will stay endemic below this threshold. Informally, we will refer to this threshold as the effective basic reproductive number denoted R_{e0}. It will describe the threshold between endemic behavior and fadeout.

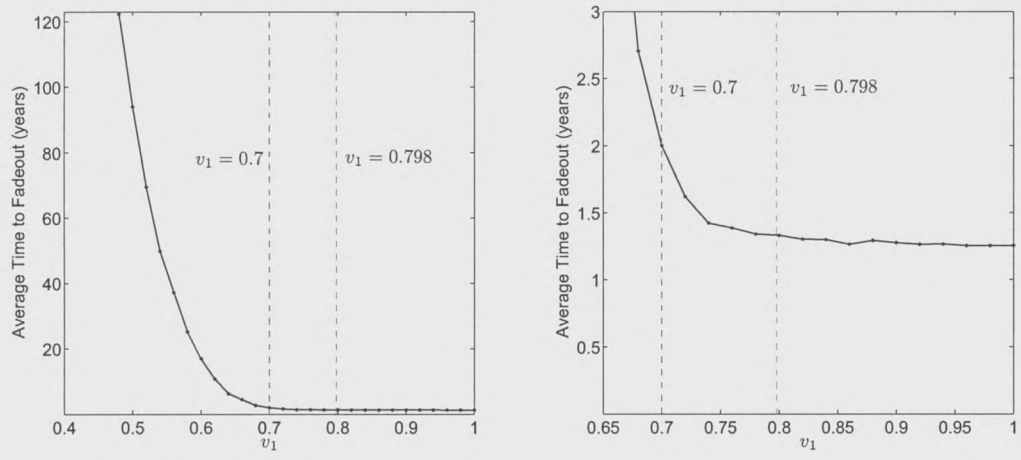

Figure 10: (a) Average fadeout time for $c_1 = 0.1$, $c_3 = 0.003$, and $v_2 = 0.9$. The red dotted lines shows the deterministic value of v_1 where the bifurcation occurs describing the change in stability from the DFE to the EE. The blue dotted line shows the value of v_1 where the average time to fadeout is two years. (b) Average fadeout time limited to three years and lower.

5.3.1 Capturing Fadeout

To capture fadeout, we will choose one of the vaccination rates and fix it at some value. Next, we fix the coupling rates, and then begin decreasing the other vaccination rate starting at the value of one. The resulting time to fadeout is then recorded. We repeat this a large number of times to obtain an average time to fadeout for each vaccination rate before it is lowered. We think of the R_{e0} as the vaccination rate where the average time to fadeout begins to increase at a rate significantly higher than previous values. Without loss of generality, we will now consider a specific example and then give the main results without detail.

Let $c_1 = 0.1$, $c_3 = 0.003$, and $v_2 = 0.9$. A bifurcation occurs at $v_1 = 0.798$ as seen in Fig. 4(b). Therefore, for any value $v_1 > 0.798$, the DFE will be stable. Simulating the FSM with the initial condition set at the EE and $(v_1, v_2) = (1, 0.9)$, we record the time to fadeout. We repeat the simulation as described five hundred times and find the average time to fadeout. Next, the vaccination rate is lowered by two percent, and the process described above is repeated. The resulting average times to fadeout are shown in Fig. 10(a). If we look closer at the lower fadeout times in Fig. 10(b), we can see an exponential increase occurring just below the deterministic value of v_1. However, the time to fadeout is still minimal and therefore and can possibly be considered as the value of R_{e0}.

One characteristic of the Fig. 10(b) to note is that it takes a little more than a year for the disease to dieout even as the vaccination rate is increased to one. This time describes how long it takes for the disease to go from the EE to DFE. Interestingly enough, this time is relatively unaffected once the vaccination rate surpasses the deterministic value of v_1 required for a stable DFE. Therefore, one conclusion we can draw is that vaccinating beyond what is deterministically predicated is unnecessary.

5.3.2 Determining the Effective Basic Reproductive Number

Although we can visually approximate reasonable values for v_1 where the average time to fadeout is sufficiently low, we want to be more thorough in defining R_{e0}. In order to do this, we will go back to our example in the previous section. Referring back to Fig. 10(b), we can see a sharper increase in the average time to fadeout occurring at $v_1 = 0.74$. For $v_1 \leq 0.74$, the average time to fadeout appears to exponentially increase. If we look at the log of this increase, we can determine a line of best fit since we expect a linear trend. Similarly, a line of best fit can be found for the fadeout times occurring with $v_1 > 0.74$. It seems reasonable to consider the data as two distinct groups, since we have seen the time to dieout predicted deterministically is essentially constant as v_1 increases. We can consider the intersection of the two lines of best fit as the critical value of $R_{e0} = v_1$ where the time to fadeout begins to exponentially increase.

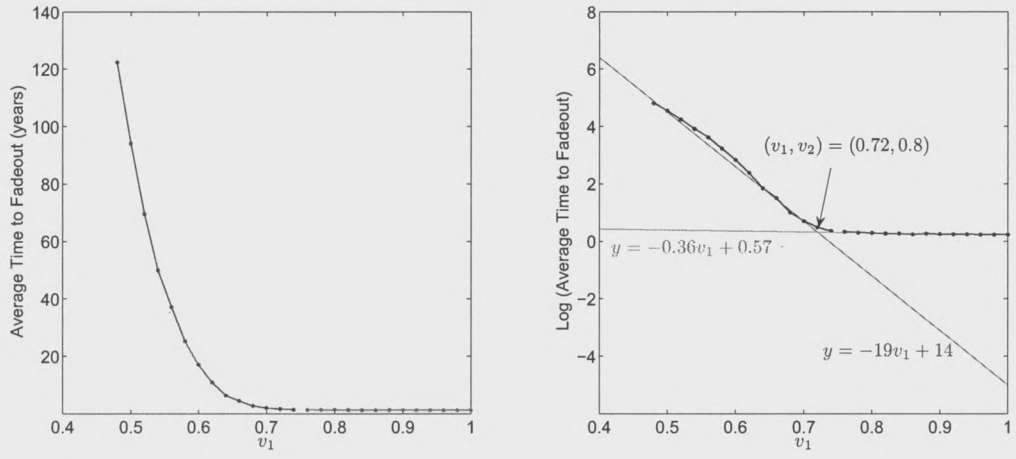

Figure 11: (a) The first collection displayed exponential growth, while the second group displayed constant behavior.(b) The lines of best fit for the log of the average fadeout time for each group.

Fig. 11(a) shows how the data was separated into an exponential and constant group. The log of each of these groups was taken in Fig. 11(b) with the corresponding lines of best fit. The value of $v_1 = 0.72$ from the intersection of the lines of best fit is the critical value where we see the average fadeout time beginning to increase exponentially.

5.3.3 Effective Reproductive Numbers Results

In this section we will give the graphical results for various changes to the linear migration and the initial fixed vaccination rate. For this section, we fix $c_3 = 0.003$. Again, we find this to be reasonable since mass action mixing is likely to occur only at the border between the northern and southern regions. Fig. 12(a-c) display the average times to fadeout for fixed values of c_1. Interestingly enough, inspection of the figures show that the average times to fadeout are not greatly affected by

Table 3: Effective Reproductive Numbers

Fixed value of c_1	Fixed value of v_2	v_1 for $R_0 = 1$	v_1 for R_{e0}
0.001	0.70	-	.712
0.001	0.75	-	.739
0.001	0.80	-	.736
0.001	0.85	.993	.734
0.001	0.90	.856	.736
0.01	0.70	-	.864
0.01	0.75	-	.750
0.01	0.80	.996	.762
0.01	0.85	.874	.740
0.01	0.90	.849	.733
0.1	0.70	.974	.721
0.1	0.75	.937	.702
0.1	0.80	.900	.720
0.1	0.85	.862	.692
0.1	0.90	.836	.763

differing values for c_1. Whereas the values of c_1 have a greater impact on the deterministic values of v_1 and v_2 to ensure a stable DFE.

Another interesting result is that when $v_2 = 0.7$, we achieve consistent fadeout in approximately two years for $v_1 \approx 0.75$ and greater. We recall, from Fig. 4, that for $v_2 = 0.7$, there is no value of $v_1 \in [0, 1]$ to ensure a stable DFE. Thus, we have a clear example of the contrast between the deterministic and stochastic approaches to analyze disease absence.

To determine the effective reproductive numbers for the variety of cases we are analyzing, we can repeat the method described in the beginning of the section by finding the intersection of the two best lines of fit for the data points that display exponential and constant behavior respectively. Omitting the details of each calculation, we collect our findings in Table 3.

Each row of Table 3 gives a comparison between the deterministic value of v_1 to ensure stability and the stochastic value of v_1 to achieve consistent fadeout in a reasonable amount of time. Similar to the previous example, for some values of c_1 and v_2, the deterministic vaccination rate v_1 needed to ensure stability is outside of the domain $[0, 1]$ yet we see consistent fadeout for a value of v_1 nonetheless.

We intuitively expected there to be a trend displaying a indirect relationship between the linear migration rate and R_{e0} since this was the case deterministically. The relationship displays more of an independent relationship, that is, increase in linear migration has little effect on R_{e0}. This is a vital difference between the deterministic and stochastic interpretations. Specifically, if only the deterministic system was taken into consideration, then predicated vaccination rates would be much higher than what is effective based on this model.

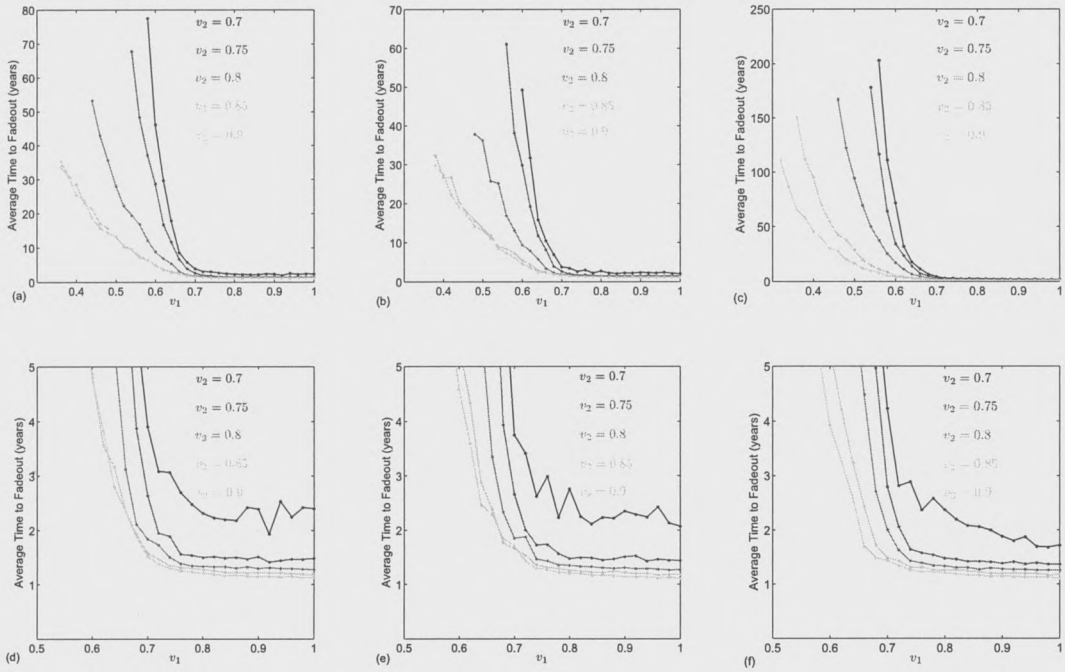

Figure 12: Average Times to Fadeout for varying linear migration rates. The rates are fixed at (a) $c_1 = 0.001$, (b) $c_1 = 0.01$, (c) $c_1 = 0.1$. The remaining three figures (d), (e), and (f) show the same displays corresponding to the figure above with an upper limit of five years for average fadeout time.

6 Summary

Beginning with the basic SIR compartmental model, we developed the theory describing the deterministic threshold for disease outbreak. The model was then extended to model long term disease dynamics by adding the effects of births and deaths. We then introduced the effects of vaccination and defined the basic reproductive number which was dependent on the vaccination rate. The models developed up to this point captured vital disease dynamics of a single population.

Next, using two types of coupling, two single population SIR models with births, deaths, and vaccinations were linked together. This model was created to reflect the disease dynamics of measles in the northern and southern regions of Cameroon. Stability of the DFE was analyzed in two separate cases; symmetric and non-symmetric vaccination. The case of symmetric vaccination showed us that linear migration has little effect on the stability of the DFE, while the opposite was true for mass action mixing. But due to the assumption of spatially uniform mixing for mass action, we concluded that its value is realistically very low. In the second case, we saw the increased linear migration rates act to enlarge the regions of stability of the DFE.

Lastly, using a stochastic representation of the coupled Cameroon model, we showed that vaccinating at rates lower than the predicted deterministic values describing a stable DFE, in fact lead to consistent disease fadeout. These lower vaccination rates were referred to as effective basic reproductive numbers. We found

the effective reproductive numbers describing reasonable fadeout time by analyzing parts of the average times to fadeout that displayed exponential and constant behavior.

Although this work has established potential useful results about the influence vaccination has on the disease dynamics of measles in Cameroon, it is important to describe a number of significant assumptions and simplifications. One of the biggest modifications is that we have ignored the exposed class for describing measles, which has a latent rate of approximately fourteen days. The primary reason for doing so was to allow for the analysis to be performed. Models that incorporate the exposed class are much more difficult to determine criterion for stability analytically. Possible future work could include this class and use more advanced numerical methods to derive results for an SEIR coupled model.

Another important limiting factor of this analysis is the accuracy of parameter values. One of the most important parameter values, the contact rate, is difficult to determine from data. It not only depends on the biological characteristics of the disease, but also on social, economic, and environmental factors that influence how individuals come in contact with one another. We have used a value that is realistic, but possibly inaccurate.

In conclusion, we have established the important differences between stochastic and deterministic analysis. Both methods were important as the deterministic work gave us foundational results about mean behavior, while the stochastic analysis then helped to find trends about disease behavior we could not have seen deterministically. It is also clear how multi-population models can capture vital dynamics inherent in the coupling. Future work could certainly include the addition of more subpopulations of Cameroon. In addition, more research about the demographics of Cameroon would lead to more accurate modeling of disease dynamics.

References

[1] N. F. Britton. *Essential Mathematical Biology.* Springer-Verlag, London, 2005.

[2] D. A. T. Cummings, W. J. Moss, K. Long, C. S. Wiysonge, T. J. Muluh, B. Kollo, E. Nomo, N. D. Wolfe, and D. S. Burke. Improved measles surveillance in Cameroon reveals two major dynamic patterns of incidence. *International Journal of Infectious Diseases*, 10(2):148–155, 2006.

[3] D. T. Gillespie. Exact Stochastic Simulation of Coupled Chemical Reactions. *The Journal of Physical Chemistry*, 81(25):2340–2361, 1977.

[4] H. W. Hethcote. The mathematics of infectious diseases. *SIAM Review*, 42(4):599–653, 2000.

[5] M. J. Keeling and P. Rohani. Estimating spatial coupling in epidemiological systems: a mechanistic approach. *Ecology Letters*, (5):20–29, 2002.

[6] W. O. Kermack and A. G. McKendrick. Contributions to the mathematical theory of epidemics. *Laboratory of the Royal College of Physicians*, 53(1-2):33–55, 1927.

[7] L. S. Liebovitch and I. B. Schwartz. Migration induced epidemics: dynamics of flux-based multipatch models. *Physics Letters A*, 332:256–267, 2004.

[8] World Health Organization. `http://www.who.org`.

[9] D. Bernoulli and S. Blower. An attempt at a new analysis of the mortality caused by smallpox and of the advantages of inoculation to prevent it. *Reviews in Medical Virology*,(14):275–288,2004.

[10] MATLAB. *Version 7.10.0 (R2010a).* The MathWorks Inc., Natick, Massachusetts, 2010.